Solvothermal Synthesis, Crystal Structure and Properties of $[Mg(en)_3][Sb_4S_7]$ – the First Thioantimonate(III) Containing a Main Group Metal Complex Cation as Structure Director

Enrique Quiroga-González, Christian Näther, and Wolfgang Bensch

Institute of Inorganic Chemistry, Christian-Albrechts-University of Kiel, Max-Eyth-Straße 2, 24118 Kiel, Germany

Reprint requests to Wolfgang Bensch. Fax: +49 431 880-1520. E-mail: wbensch@ac.uni-kiel.de

Z. Naturforsch. **2009**, *64b,* 1312 – 1318; received October 1, 2009

Dedicated to Professor Hubert Schmidbaur on the occasion of his 75th birthday

The new thioantimonate $[Mg(en)_3][Sb_4S_7]$ containing for the first time a $[Mg(en)_3]^{2+}$ cation as structure-directing unit was synthesized under solvothermal conditions applying elemental Mg, $SbCl_3$, S and ethylenediamine. The compound crystallizes in the monoclinic space group $P2_1/c$ with a = 9.9267(6), b = 14.254(1), c = 17.259(1) Å, β = 102.611(7)°, V = 2383.1(3) Å^3, Z = 4. In the structure trigonal SbS_3 pyramids are joined to form an Sb_3S_3 ring. The rings are connected through SbS_3 units yielding an undulated chain anion running along [001]. Considering so-called secondary Sb–S bonds, a layer-like thioantimonate anion is formed. The $[Mg(en)_3]^{2+}$ cations are located between the layers. Relatively short S···H–N contacts suggest hydrogen bonding interactions between the cation and the $[Sb_4S_7]^{2-}$ anion. The compound starts to decompose at about 220 °C. The optical band gap of 2.35 eV is in agreement with the orange color of the crystals. In the Raman spectrum prominent Sb–S resonances are seen between 250 and 400 cm^{-1} which can be assigned to different Sb–S vibrations.

Key words: Thioantimonate, Solvothermal Syntheses, Crystal Structure, Spectroscopic Properties

Introduction

The chemistry of thioantimonates(III) is characterized by a large variety of chemical compositions, primary and secondary building units (SBU) and dimensionalities of the thioantimonate networks. The latter is caused by a very flexible and hierarchical interconnection of the SBU, yielding different dimensionalities of the inorganic network even for a given Sb : S ratio [1 – 3]. An interesting aspect of the thioantimonate chemistry is the occurrence of mixed-valence Sb(III)/Sb(V) compounds like in $[Ni(dien)_2]_2Sb_4S_9$ [4]. Among the different Sb : S ratios observed in thioantimonate(III) compounds, the $[Sb_4S_7]^{2-}$ anion with Sb : S = 1 : 1.75 is the most common one. Until now about 40 compounds containing this anion have been reported [1, 3, 5 – 24]. Of special interest are open-framework thioantimonates with accessible empty voids, cages or holes. If small molecules within the voids in these frameworks can be exchanged, changes of the physical properties may be induced leading to potential applications as sensors, for example [25]. However, the interaction between the structure-directing molecules or cations with the negatively charged thioantimonate networks is strong and thus preventing the removal of the guests without collapse of the structures. An interesting synthetic approach is to pillar layered thioantimonates(III) with organic structure-directing molecules or metal complexes [26]. However, the successful pillaring of the layers depends on different factors like the thermal stability of the pillar under solvothermal conditions.

In the presence of organic ammonium cations S···H hydrogen bonding interactions play an important role. Compared to O···H or F···H bonds the strength of an individual S···H bond is significantly lower, but most thioantimonates(III) with such cations display a large number of such bonds, and therefore they cannot be neglected. Very often, the S···H bonding interaction leads to fully ordered NH_3 groups, and in most compounds the NH_3 group exhibits a special arrangement

0932–0776 / 09 / 1100–1312 $ 06.00

with respect to the S atoms of the thioantimonate network [27 – 30].

An example for a three-dimensional thioantimonate network is $K_2Sb_4S_7$ [6]. For most of the $[Sb_4S_7]^{2-}$-containing compounds the well-known counterion size effect is observed: large cations favor the formation of layers and/or chains. Large organic ammonium cations force the crystallization of layered compounds, and depending on the size and orientation of the cation, large interlayer separations are observed like 6.56 Å for $(C_2H_5NH_3)_2Sb_4S_7$ [16] or 9.90 Å for $(CH_3(CH_2)_4NH_3)_2Sb_4S_7$ [1]. The solvothermal synthesis method is most suitable for the preparation of thioantimonates(III). Many compounds were obtained using transition metal complexes either as starting material, or they are formed by *in situ* reaction between transition metal cations and the amine supplied as structure director and solvent [31 – 37]. Until now no thioantimonates(III) containing a main group metal complex cation as structure-directing unit have been reported. In our ongoing work we explored the possibility of using group 2 metal complexes for the synthesis of new thioantimonates(III). In this paper we report the solvothermal synthesis, crystal structure and some selected properties of the first alkaline-earth metal complex-containing thioantimonate(III), $Mg(en)_3[Sb_4S_7]$.

Experimental Section

Synthesis

Mg (0.164 mmol), $SbCl_3$ (0.328 mmol) and S (0.657 mmol) were mixed with 5 mL of ethylenediamine in a 35 mL teflon-lined stainless-steel autoclave. The sealed vessel was heated at 170 °C for 10 d. After cooling to r. t., the product was filtered off and washed with water, ethanol and acetone. Large plate-like orange crystals were obtained in a yield close to 100 % based on Sb. Attempts to synthesize the analogous Ca and Sr compounds were not successful despite a large variation of the reaction parameters. Chemical analysis: calcd. N 9.17, C 8.86, H 2.94, S 23.5; found N 10.1, C 9.39, H 3.03, S 23.79 %.

Single-crystal structure analysis

The data were measured using an Imaging Plate Diffraction System (Stoe & Cie IPDS1) with MoK_α radiation. The structure was solved with Direct Methods using SHELXS-97 [38] and refined with SHELXL-97 [38]. All non-hydrogen atoms were refined with anisotropic displacement parameters. All hydrogen atoms were positioned with idealized geometry and refined isotropically using a riding model. Selected crystal structure data and results of the structure refinement are shown in Table 1.

Table 1. Crystal structure data and refinement results of $[Mg(en)_3][Sb_4S_7]$.

Empirical formula	$C_6H_{24}MgN_6S_7Sb_4$
M_r, g mol^{-1}	916.04
Crystal size, mm^{-1}	$0.15 \times 0.11 \times 0.07$
Crystal system	monoclinic
Space group	$P2_1/c$
a, Å	9.9267(6)
b, Å	14.254(1)
c, Å	17.259(1)
β, deg	102.611(7)
V, Å^3	2383.1(3)
T, K	170
Z	4
D_{calc}, g cm^{-3}	2.55
2θ range, deg	5 – 56
μ (MoK_α), mm^{-1}	5.1
hkl range	−12/13; −18/18; −22/22
Refl. meas. / indep. / R_{int}	34189 / 5744 / 0.0372
Refl. with $I \geq 2\sigma(I)$	5522
Ref. parameters	218
$R1$ $[I \geq 2\sigma(I)]$/$wR2$ [all data]	0.0294 / 0.0794
Goof	0.970
$\Delta\rho_{fin}$ (max/min), e Å^{-3}	1.22 / −1.36

CCDC 752314 contains the supplementary crystallographic data for this paper. These data can be obtained free of charge from The Cambridge Crystallographic Data Centre *via* www.ccdc.cam.ac.uk/data_request/cif.

DTA-TG measurements

DTA-TG measurements were performed in Al_2O_3 crucibles using a STA-409CD thermobalance (Netzsch). The measurements were performed in Al_2O_3 crucibles under a nitrogen atmosphere with a heating rate of 4 °C min^{-1}.

X-Ray powder diffractometry

The homogeneity of the product was checked with X-ray powder patterns, which were recorded on a Stoe STADI P diffractometer (Ge monochromator, CuK_α radiation, λ = 1.54056 Å).

Raman spectroscopy

Raman spectra were recorded in the region 100 – 3500 cm^{-1} with a Bruker IFS 66 Fourier Transform Raman spectrometer (wavelength: 541.5 nm).

UV/Vis spectroscopy

UV/Vis spectroscopic investigations were conducted at r. t. using a UV/Vis-NIR two-channel spectrometer Cary 5 (Varian Techtron Pty., Darmstadt). The optical properties of

the compound were investigated by studying the UV/Vis reflectance spectrum of the powdered sample. The absorption data were calculated with the Kubelka-Munk relation for diffuse reflectance data. $BaSO_4$ powder was used as reference material.

Scanning electron microscopy (SEM)/energy dispersive X-ray fluorescence (EDX)

EDX analyses were done with a Philips ESEM XL30 instrument equipped with an EDAX detector.

Elemental analysis

CHN analysis was performed using a Euro EA Elemental Analyzer (Euro Vector Instruments and Software).

Results and Discussion

The title compound crystallizes in the monoclinic space group $P2_1/c$ (Table 1) with all atoms being located on general positions. The primary building units are four trigonal SbS_3 pyramids (Fig. 1). Three SbS_3 units (Sb1, Sb3 and Sb4) share common corners to form a six-membered Sb_3S_3 heteroring. These rings are joined by the $Sb(2)S_3$ pyramids yielding a chain comprised of alternating Sb_3S_3 rings and $Sb(2)S_3$ pyramids running along [001] (Fig. 2). The chain proceeds in a zig-zag-like fashion. The Sb–S bond lengths are between 2.3302(10) and 2.5095(9) Å (Table 2) which are typical for thioantimonates(III) [1 – 26]. The two shortest Sb–S bonds (Sb(2)–S(2): 2.3302(10) and Sb(4)–S(7): 2.3962(9) Å) are observed to the terminal S atoms suggesting stronger bonds. The S–Sb–S angles (Table 2) (86.44(3)–101.76(3)°) indicate a distortion from the ideal trigonal-pyramidal geometry which is often observed in thioantimonate(III) compounds. The chains are arranged in a way that the Sb_3S_3 rings point toward the pocket formed by the $Sb(2)S_3$ pyramid joining two adjacent rings (Fig. 2).

Like in many other thioantimonates(III), the Sb(III) ions in the title compound have next-nearest S neighbors at distances above 3 Å but below the sum of the van der Waals radii of Sb and S of about 3.8 Å. In $[Mg(en)_3][Sb_4S_7]$ the so-called secondary bonds are between 3.061 and 3.582 Å. Considering these weak interactions the coordination environments of Sb(1), Sb(3), and Sb(4) are enhanced to five and six, respectively, whereas Sb(2) is not involved in such contacts (Fig. 3). The resulting $Sb(4)S_6$ unit may be viewed

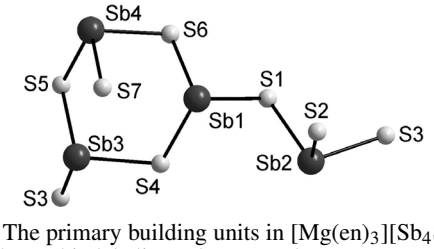

Fig. 1. The primary building units in $[Mg(en)_3][Sb_4S_7]$ with crystallographic labeling scheme used.

Table 2. Selected bond lengths (Å) and angles (deg)[a].

Sb(1)-S(6A)	2.4356(8)	Sb(3)-S(5)	2.4733(9)
Sb(1)-S(1)	2.5011(9)	Sb(3)-S(4)	2.4759(9)
Sb(1)-S(4A)	2.5048(9)	Sb(3)-S(3)	2.5069(9)
Sb(2)-S(2)	2.3302(10)	Sb(4)-S(7)	2.3962(9)
Sb(2)-S(3)	2.4742(9)	Sb(4)-S(5)	2.4969(9)
Sb(2)-S(1)	2.5095(9)	Sb(4)-S(6)	2.4986(9)
S(6A)-Sb(1)-S(1)	87.11(3)	S(7)-Sb(4)-S(5)	94.89(3)
S(6A)-Sb(1)-S(4A)	100.04(3)	S(7)-Sb(4)-S(6)	95.99(3)
S(1)-Sb(1)-S(4A)	93.90(3)	S(5)-Sb(4)-S(6)	91.57(3)
S(2)-Sb(2)-S(3)	99.19(3)	S(5)-Sb(3)-S(4)	99.85(3)
S(2)-Sb(2)-S(1)	101.76(3)	S(5)-Sb(3)-S(3)	86.44(3)
S(3)-Sb(2)-S(1)	93.00(3)	S(4)-Sb(3)-S(3)	91.23(3)
Mg(1)-N(21)	2.193(3)	Mg(1)-N(2)	2.201(3)
Mg(1)-N(1)	2.194(3)	Mg(1)-N(22)	2.218(3)
Mg(1)-N(12)	2.194(3)	Mg(1)-N(11)	2.224(3)
N(21)-Mg(1)-N(1)	91.11(13)	N(12)-Mg(1)-N(22)	94.03(13)
N(21)-Mg(1)-N(12)	98.72(13)	N(2)-Mg(1)-N(22)	94.44(13)
N(1)-Mg(1)-N(12)	168.16(15)	N(21)-Mg(1)-N(11)	94.40(13)
N(21)-Mg(1)-N(2)	167.61(14)	N(1)-Mg(1)-N(11)	93.22(14)
N(1)-Mg(1)-N(2)	78.86(13)	N(12)-Mg(1)-N(11)	79.55(12)
N(12)-Mg(1)-N(2)	92.13(13)	N(2)-Mg(1)-N(11)	93.43(13)
N(21)-Mg(1)-N(22)	78.93(12)	N(22)-Mg(1)-N(11)	170.02(13)
N(1)-Mg(1)-N(22)	94.32(15)		

[a] Symmetry transformations used to generate equivalent atoms: A = $x, -y+3/2, z+1/2$.

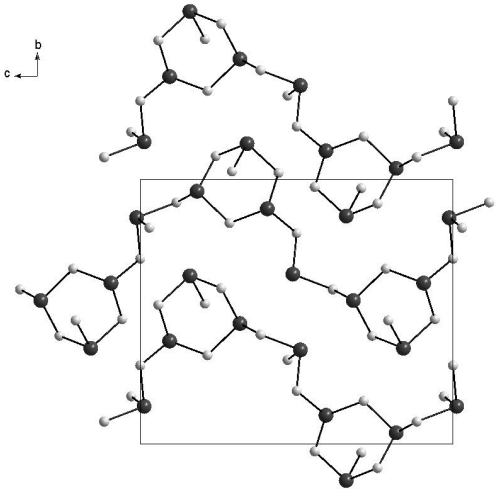

Fig. 2. The $[Sb_4S_7]^{2-}$ chains in the title compound running along [001].

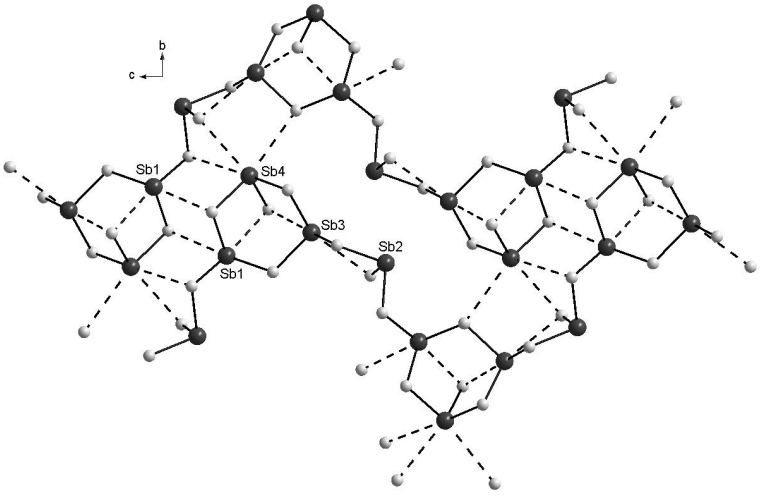

Fig. 3. The thioantimonate anion of $[Mg(en)_3][Sb_4S_7]$ with the so-called secondary Sb–S bonds drawn as broken lines.

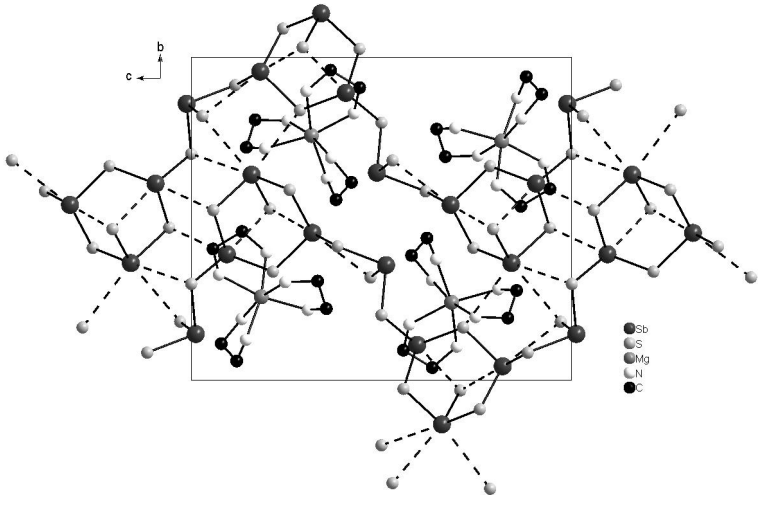

Fig. 4. Arrangement of the $[Mg(en)_3]^{2+}$ cations and the $[Sb_4S_7]^{2-}$ anions. Note that broken lines indicate long Sb–S contacts. H atoms are not shown.

as a strongly distorted octahedron with two short and two long equatorial and one short and one long axial Sb–S distance. The two SbS_5 polyhedra may be described as distorted trigonal bipyramids. These secondary Sb–S bonds join the primary structural units into larger building blocks. The Sb(1)–S(7) (3.0606 Å) and Sb(3)–S(7) (3.0696 Å) contacts transform the Sb_3S_3 ring into a Sb_3S_4 unit with a geometry often called semi-cube, which is a structural motif frequently observed in extended thioantimonate(III) structures.

Moreover, layers extending in the (100) plane are generated by the weak Sb–S contacts. The layered anions are stacked onto each other along [100] with relatively large, nearly rectangular openings composed of eight Sb and eight S atoms (Sb_8S_8) forming tunnels also directed along [100] (Fig. 3). Another special structural feature of the layer is the occurrence of a cluster-like configuration of three Sb_3S_4 semi-cubes (Fig. 3).

The Mg^{2+} cation in the charge-compensating complex $[Mg(en)_3]^{2+}$ is in a distorted octahedral environment of six N atoms of three ethylenediamine molecules, and the conformation of the complex is $\Delta(\lambda\lambda\delta)$. The Mg–N bond lengths (Table 2) range from 2.193(3) to 2.224(3) Å, which are typical values found in the literature [39]. Notably, the $[Mg(en)_3]^{2+}$ unit has only been structurally characterized in two compounds [39]. The N–Mg–N an-

Table 3. Hydrogen bond geometry of $[Mg(en)_3][Sb_4S_7]$. Distances in Å and angles in deg.

D–H	d(H···A)	⟨D–H···A	d(D···A)	A (symm. operation)
N1–H1B	2.68	127.6	3.32	S2 ($x-1$, $-y+3/2$, $z-1/2$)
N2–H2C	2.51	165.2	3.41	S4
N2–H2D	2.88	125.0	3.49	S3
N11–H11A	2.77	155.8	3.63	S5 ($-x+1$, $y+1/2$, $-z+1/2$)
N11–H11B	2.65	168.2	3.55	S7 ($x-1$, y, z)
N12–H12C	2.77	164.4	3.66	S3
N12–H12D	2.61	155.7	3.47	S7 ($-x+2$, $y+1/2$, $-z+1/2$)
N21–H21C	2.54	167.5	3.45	S2 ($x-1$, $-y+3/2$, $z-1/2$)
N21–H21D	2.65	142.0	3.42	S5 ($-x+1$, $y+1/2$, $-z+1/2$)
N22–H22A	2.82	149.5	3.64	S7 ($-x+2$, $y+1/2$, $-z+1/2$)
N22–H22B	2.68	158.7	3.55	S1 (x, $-y+3/2$, $z-1/2$)

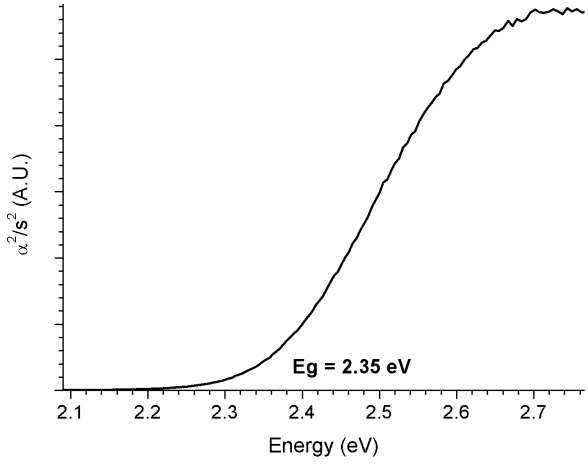

Fig. 5. The UV/Vis diffuse reflectance spectrum of the title compound.

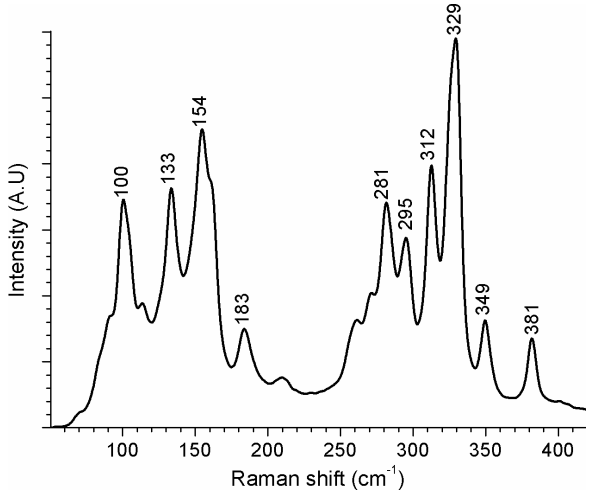

Fig. 6. The Raman spectrum of $[Mg(en)_3][Sb_4S_7]$.

gles indicate a severe distortion with values between 78.86(13) and 170.02(13)°, and *trans* angles of 167.61(14) to 170.02(13)°. In the isostructural compounds $[M(en)_3]Sb_4S_7$ (M = Ni, Fe, Co) the conformation of the cations are either $\Delta(\lambda\lambda\lambda)$ or $\Lambda(\delta\delta\delta)$ [13–15], in contrast to what is observed in the title compound. The $\Delta(\lambda\lambda\lambda)$ or $\Lambda(\delta\delta\delta)$ conformations around the M^{2+} ions also leads to distortions of the octahedral environments with *trans* N–M–N angles of 162–165° for Mn^{2+}, 169–170° for Co^{2+}, and 170–171° for Ni^{2+}.

The $[Mg(en)_3]^{2+}$ cations are positioned between the anionic thioantimonate(III) layers and are located above and below the periphery of the rectangular rings (Fig. 4).

Eleven of the twelve H atoms bonded to N atoms and six out of the seven S atoms are involved in H bonding interactions (Table 3). Although S···H bonds are weak, the large number of such interactions leads to a significant contribution to the stability of the compounds. Transition metal-containing counterions in thioantimonates(III) are very often located and oriented in a way to the anionic network that optimal H bonding interactions are possible. Hence, such cations are mainly located above or below large rings formed by Sb and S atoms. The inter-layer spacing of 6.55 Å in $[Mg(en)_3][Sb_4S_7]$ is very similar to those reported for the isostructural compounds mentioned above (Mn^{2+}: 6.65 Å; Co^{2+}: 6.56 Å; Ni^{2+}: 6.55 Å).

The thermal stability of $[Mg(en)_3][Sb_4S_7]$ was investigated by DTA-TG experiments performed in N_2 atmosphere. Above about 220 °C the emission of the en ligands starts, and the thermal decomposition reaction is accompanied by an intense endothermic signal in the DTA curve. The decomposition is finished at about 350 °C, and in the grey residue only the reflections of Sb_2S_3 could be observed in the X-ray powder pattern. However, since several reflections of MgS and Sb_2S_3 overlap, and the scattering power of Mg is much lower than that of Sb, the presence of MgS in the thermal decomposition product could not be proven unambiguously by powder diffractomery.

The optical band gap of the compound was determined by diffuse UV/Vis reflectance measurements (Fig. 5). The observed value of about 2.35 eV is in good agreement with the orange color of the compound. The metal cation seems to have no significant influence on the optical band gap because similar values were reported for Ni^{2+} (2.35 eV) and Fe^{2+} (2.25 eV), indicating that M^{2+}-based electronic states are not heavily involved in the electronic transition.

The Raman spectrum of the title compound is displayed in Fig. 6. The typical resonances of the SbS_x (x = 3 – 6) stretching vibrations occur between 250 and 400 cm^{-1}. In the present spectrum several intense signals are located in this region. On the basis of literature data [40] the bands located at 349 and 329 cm^{-1} are tentatively assigned to the stretching vibrations of the SbS_3 pyramid. In $(CuI_2)Cu_3SbS_3$ containing an isolated $[SbS_3]^{3-}$ anion these resonances occur at 362 and 339 cm^{-1}, whereas a prominent shift of about 60 cm^{-1} to lower frequencies was reported for SbS_6 and SbS_7 units in $MnSb_2S_4$ [41, 42]. According to the assignment of the bands in the Raman spectrum of $[Cr(tren)SbS_3]\cdot H_2O$ (tren = tris(2-aminoethyl)amine) the resonance at about 281 cm^{-1} may be caused by an asymmetric S–Sb–S stretching mode. The signals at 312 and 295 cm^{-1} may be due to the weak bonding interactions between the Sb(III) ions and the next-nearest S atoms [41, 42]. Resonances located at about 320 and 290 cm^{-1} were explained with the presence of SbS_5 units displaying the typical bonding pattern of three short and two long secondary bonds [41, 42]. As discussed above two Sb atoms in the title compound are in a $3+2$ environment of S atoms, and therefore the two resonances at 312 and 296 cm^{-1} may be caused by these two SbS_5 groups. The signature of the SbS_6 unit may also occur in this region and/or participates in these two low-energy bands. Further assignment of the remaining resonances is difficult because lattice vibrations are also located in the region below about 250 cm^{-1}.

Conclusions

The new thioantimonate(III) $[Mg(en)_3][Sb_4S_7]$ was obtained as orange crystals in almost quantitative yield under solvothermal conditions and represents the first thioantimonate(III) containing a main group metal complex as structure-directing unit. The compound belongs to the group of thioantimonates(III) with an Sb : S ratio of 1 : 1.75 for which the largest number of examples was reported in the literature. The $[Sb_4S_7]^{2-}$-containing compounds can be classified according to their dimensionalities and/or space groups [3]. With the title compound nine structurally characterized $[M(L)][Sb_4S_7]$ (L = ligand) compounds crystallizing in space groups $P2_1/c$ are known. For the compounds containing cations which are surrounded by the less bulky ligand diethylenetriamine a layered thioantimonate network is observed, whereas the more space-demanding $[M(en)_3]^{2+}$ complexes force the formation of a chain anion. Hence, the structure of the title compound is another example supporting the postulated relation between cation size and dimensionality of the thiometalate anion.

Acknowledgement

Financial support by the State of Schleswig-Holstein and the Fonds der Chemischen Industrie is gratefully acknowledged.

[1] A. Puls, M. Schaefer, C. Näther, W. Bensch, A. V. Powell, S. Boissière, A. M. Chippindale, *J. Solid State Chem.* **2005**, *178*, 1171 – 1181.
[2] A. Puls, C. Näther, R. Kiebach, W. Bensch, *Solid State Sci.* **2006**, *8*, 1085 – 1097.
[3] H. Lühmann, Z. Rejai, K. Möller, P. Leisner, M.-E. Ordolff, C. Näther, W. Bensch, *Z. Anorg. Allg. Chem.* **2008**, *634*, 1687 – 1695.
[4] R. Stähler, B.-D. Mosel, H. Eckert, W. Bensch, *Angew. Chem.* **2002**, *114*, 4671 – 4673; *Angew. Chem. Int. Ed.* **2002**, *41*, 4487 – 4489.
[5] M. Zhang, T. L. Sheng, X. H. Huang, R. B. Fu, X. Wang, S. M. Hu, S. C. Xiang, X. T. Wu, *Eur. J. Inorg. Chem.* **2007**, 1606 – 1612.
[6] H. A. Graf, H. Schäfer, *Z. Naturforsch.* **1972**, *27b*, 735 – 739.
[7] G. Dittmar, H. Schäfer, *Z. Anorg. Allg. Chem.* **1977**, *437*, 183 – 187.
[8] G. Dittmar, H. Schäfer, *Z. Anorg. Allg. Chem.* **1978**, *441*, 93 – 97.
[9] G. Dittmar, H. Schäfer, *Z. Anorg. Allg. Chem.* **1978**, *441*, 98 – 102.
[10] B. Eisenmann, H. Schäfer, *Z. Naturforsch.* **1979**, *34b*, 383 – 385.
[11] G. Cordier, H. Schäfer, C. Schwidetzky, *Z. Naturforsch.* **1984**, *39b*, 131 – 134.
[12] W. S. Sheldrick, H.-J. Häusler, *Z. Anorg. Allg. Chem.* **1988**, *557*, 105 – 111.

[13] H.-O. Stephan, M. G. Kanatzidis, *Inorg. Chem*. **1997**, *36*, 6050 – 6057.
[14] W. Bensch, M. Schur, *Z. Naturforsch.* **1997**, *52b*, 405 – 409.
[15] P. Vaqueiro, D. P. Darlow, A. M. Chippindale, A. V. Powell, *Solid State Ionics* **2004**, *172*, 601 – 605.
[16] M. Schur, W. Bensch, *Eur. J. Solid State Inorg. Chem*. **1997**, *34*, 457 – 466.
[17] R. Stähler, C. Näther, W. Bensch, *J. Solid State Chem*. **2003**, *174*, 264 – 275.
[18] M. Schaefer, D. Kurowski, A. Pfitzner, C. Näther, W. Bensch, *Acta Crystallogr*. **2004**, *E60*, m183–m185.
[19] V. Spetzler, C. Näther, W. Bensch, *Z. Naturforsch.* **2006**, *61b*, 715 – 720.
[20] M. Schaefer, R. Stähler, W.-R. Kiebach, C. Näther, W. Bensch, *Z. Anorg. Allg. Chem.* **2004**, *630*, 1816 – 1822.
[21] R. Kiebach, A. Griebe, C. Näther, W. Bensch, *Solid State Sci.* **2006**, *8*, 541 – 547.
[22] A. V. Powell, R. J. E. Lees, A. M. Chippindale, *Inorg. Chem*. **2006**, *45*, 4261 – 4267.
[23] F. Q. Huang, J. A. Ibers, *J. Solid State Chem*. **2005**, *178*, 212 – 217.
[24] J. Zhou, J. Dai, G.-Q. Bian, C.-Y. Li, *Coord. Chem. Rev*. **2009**, *253*, 1221 – 1247.
[25] G. A. Ozin, *Supramolecular Chem*. **1995**, *6*, 125 – 134.
[26] R. Kiebach, R. Warratz, C. Näther, W. Bensch, *Z. Anorg. Allg. Chem.* **2009**, *635*, 988 – 994.
[27] L. Engelke, C. Näther, W. Bensch, *Eur. J. Inorg. Chem*. **2002**, 2936 – 2941.
[28] M. Schur, A. Gruhl, C. Näther, I. Jess, W. Bensch, *Z. Naturforsch.* **1999**, *54b*, 1524 – 1528.
[29] M. Schur, W. Bensch, *Z. Naturforsch*. **2002**, *57b*, 1 – 7.
[30] V. Spetzler, H. Rijnberk, C. Näther, W. Bensch, *Z. Anorg. Allg. Chem*. **2004**, *630*, 142 – 148.
[31] R. Kiebach, W. Bensch, R. D. Hoffmann, R. Pöttgen, *Z. Anorg. Allg. Chem*. **2003**, *629*, 532 – 538.
[32] M. Schur, H. Rijnberk, C. Näther, W. Bensch, *Polyhedron* **1998**, *18*, 101 – 107.
[33] M. Schaefer, C. Näther, W. Bensch, *Solid State Sci*. **2003**, *5*, 1135 – 1139.
[34] M. Schaefer, C. Näther, N. Lehnert, W. Bensch, *Inorg. Chem*. **2004**, *43*, 2914 – 2921.
[35] R. Stähler, C. Näther, W. Bensch, *J. Solid State Chem*. **2003**, *174*, 264 – 275.
[36] R. Stähler, W. Bensch, *Z. Anorg. Allg. Chem*. **2002**, *628*, 1657 – 1662.
[37] R. Kiebach, F. Studt, C. Näther, W. Bensch, *Eur. J. Inorg. Chem*. **2004**, 2553 – 2556.
[38] G. M. Sheldrick, SHELXS/L-97, Programs for Crystal Structure Determination, University of Göttingen, Göttingen (Germany) **1997**. See also: G. M. Sheldrick, *Acta Crystallogr.* **2008**, *A64*, 112 – 122.
[39] A. F. Waters, A. H. White, *Aust. J. Chem.* **1996**, *49*, 61 – 72.
[40] K. Möller, C. Näther, A. Bannwarth, W. Bensch, *Z. Anorg. Allg. Chem.* **2007**, *633*, 2635 – 2640
[41] A. Pfitzner, D. Kurowski, *Z. Kristallogr*. **2000**, *215*, 373 – 376.
[42] A. Pfitzner, *Chem. Eur. J.* **1997**, *3*, 2032 – 2038.